shift on the phenyl protons of oxidized Fe^{III}TPPCl and suggest that it could arise from A_{2u} symmetry of a π cation radical species. In addition, they have shown that the near-IR bands are quite similar to ZnTPP radical species and that the first wave electrochemical potential for oxidation is independent of axial ligands for Fe^{III}TPP$^+$. If this radical is formed, it must be strongly antiferromagnetically coupled to the Fe(III) iron.[30] In general, the formation of simple π cation radicals of metalloporphyrins of TTP result in a weaker, broadened, and blue-shifted Soret band with increased absorbance over the 600–700-nm range.[36] Peterson et al.[19] reported an excited-state band at 370 nm of [Fe^{III}TPP]$_2$O in both benzene and pyridine. These transient absorption studies were attributed to formation of a Fe(III) porphyrin radical. In the absence of a good coordinating base, it was proposed that a π cation radical species was observed rather than an Fe(IV) disproportionation complex. The appearance of a band at ~370 nm was also seen in the present studies, but we do not observe a clear change in the difference spectra of the [Fe^{III}TPP]$_2$O in the 600–700-nm range; however, it is possible that a strongly coupled Fe(III) high spin state to a π cation radical may alter the expected shifts. It may be pointed out, however, that coupling between copper and the π cation radical of Cu^{II}TPP in electrochemical oxidation still gives the features of a π cation radical.[36]

Conclusion

The photoexcitation of [Fe^{III}TPP]$_2$O at either 532 or 355 nm results in an intermediate state with a lifetime of <100 ps that may be an excited state localized to a monomer unit and that forms the photodissociated pair TPPFe^{II+} + TPPFe^{III}–O$^-$ with smaller yield photodisproportionation reaction, which generates Fe^{II}TPP and TPPFe^{IV}=O. In the absence of easily oxidizable substrates, the photoproducts recombine into [Fe^{III}TPP]$_2$O within 4.3 ns.

Acknowledgment. This research was supported in part by the Veterans Administration Medical Center.

Registry No. [Fe^{III}TPP]$_2$O, 12582-61-5; TPPFe^{II+}, 29484-63-7; TPP-Fe^{III}—O$^-$, 115162-51-1; Fe^{II}TPP, 16591-56-3; TPPFe^{IV}=O, 84152-32-9.

---

(35) Goff, H. M.; Phillippi, M. A.; Boersma, A. D.; Hansen, A. P. In *Electrochemical and Spectrochemical Studies in Biological Redox Components*; Kadish, K. M., Ed.; ACS Advances in Chemistry Series 201; American Chemical Society: Washington, DC, 1982; pp 357–376.

(36) Dolphin, D.; Muljiani, Z.; Rousseau, K.; Borg, D. C.; Fajer, J.; Felton, R. H. *Ann. N.Y. Acad. Sci.* **1973**, *206*, 177–197.

Trends in the Optical Signatures for Transition-Metal Oxide Carbonyl Complexes. Evaluation of Transition-Metal Carbonyl, M(CO)$_x$, Binding Energies

M. J. McQuaid, K. Morris, and J. L. Gole*

Contribution from the High Temperature Laboratory Center for Atomic and Molecular Science and School of Physics, Georgia Institute of Technology, Atlanta, Georgia 30332.

Received October 19, 1987

Abstract: Transition-metal atoms entrained in argon, helium, and CO are oxidized with ozone (O$_3$) and nitrogen dioxide (NO$_2$) to study the nature of the metal atom complexation with CO. We establish a method for evaluating M–CO binding energies through comparison of the chemiluminescent emission from the oxidation of argon- and CO-entrained transition-metal atoms. These studies have thus far yielded $E_{\text{binding}}(\text{Ti(CO)}_x) \approx 1.75$ eV and $E_{\text{binding}}(\text{NiCO}) \approx 1.10$ eV, the latter in excellent agreement with previous experimental and theoretical evaluations of the Ni–CO bond energy. We identify the optical signatures for transition-metal oxide carbonyl (MOCO) complexes formed in the oxidation of M(CO) complexes. We outline trends in the nature of the observed metal oxide complex emissions. The current study suggests a method for obtaining the spectra of transition-metal carbonyl (M(CO)$_x$, $x = 1, 2$) complexes.

The volatile metal carbonyls ligated with several carbonyl groups exhibit a variety of molecular structures. These structures have created much previous interest, and the vibrational spectroscopy of the multiply ligated species, primarily those of the transition metals, which play an extremely important role in chemistry, have been the subject of considerable investigation. Both M–C and C–O stretching modes have been well studied.[1] While there has been considerable research in the volatile multiply ligated metal carbonyls, relatively little experimental work has focused on the basic metal monocarbonyl, M–CO, binding energies and MCO spectroscopy is sparse.[2] This gap in understanding is significant, for, without doubt, the most celebrated and studied gas–surface interaction is that of carbon monoxide on metal surfaces.[3]

The metal surface–CO interaction has been the subject of innumerable studies employing a wide variety of experimental[2] and theoretical methods.[3-5] These studies have been, in large part, a response to the industrial versatility of methods running the gamut from methanol formation[6] to the Fisher–Tröpsch synthesis.[7] MCO molecules, where M is a transition-metal element, have been of considerable interest as prototypes for CO chemisorption on metal surfaces. There are now a large number of theoretical papers concerning the electronic and bonding properties of these species, the proliferation of approaches to the study of NiCO being especially notable.[8] Much less experimental

---

(1) See references in: Nakamoto, K. *Infrared Spectra of Inorganic and Coordination Compounds*; Wiley: New York, 1972.

(2) Somorjai, G. A. *Chemistry in Two Dimensions: Surfaces*; Cornell University: Ithaca, NY, 1981, references contained therein. Poliakoff, M.; Weitz, E. *Acc. Chem. Res.* **1987**, *20*, 408–414, and references cited therein.

(3) Allison, J. N.; Goddard, W. A., III *Surf. Sci.* **1982**, *115*, 553.

(4) Parra, Z.; Micha, D. A. *Chem. Phys. Lett.* **1986**, *132*, 488.

(5) Richardson, N. V.; Bradshaw, A. M. *Surf. Sci.* **1979**, *88*, 255.

(6) Kilar, K. *Adv. Catal.* **1982**, *31*, 243.

(7) Fischer, F.; Tropsch, H. *Brennst.-Chem.* **1926**, *7*, 97. Vannice, M. A. *Catal. Rev.—Sci. Eng.* **1976**, *14*, 153.

0002-7863/88/1510-5280$01.50/0

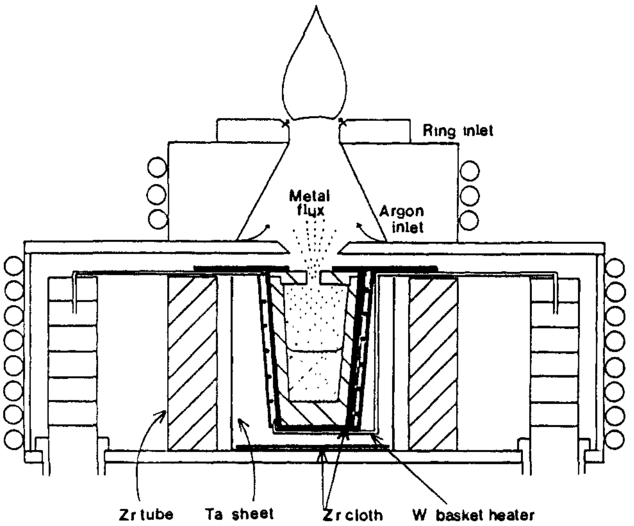

Figure 1. Schematic of metal entrainment-agglomeration oxidation device showing tungsten basket heater, insulation, entrainment region, and oxidation region.

data have been obtained, mostly from rare-gas matrix studies.[9,10] In addition, despite their potential mimicry of molecules adsorbed on metals, there have been relatively few matrix studies of ligands bonded to very small matrix-isolated metal clusters. The systems Ni–CO,[11] Cu–CO,[12] and Pd–CO[13] have been studied more or less systematically.[10] However, these studies and the structural interpretation of observed spectra have been inconclusive.

Table I. Comparative System Parameters for the Oxidation of Argon- and CO-Entrained Transition-Metal Atoms

reactive system[a]	estd flux to reactn zone,[b] atoms/cm^2·s	approx entrainment gas pressure, Torr	figure
Sc in Ar + NO_2	$\sim 2 \times 10^{16}$–2×10^{17}	~ 0.8[c]	9a
Sc in CO + NO_2	$\sim 2 \times 10^{16}$–2×10^{17}	~ 1[c]	9b
Ti in Ar + O_3	vaporization from filament with entrainment	~ 2[d]	2a
Ti in CO + O_3		~ 2.5[d]	2b
V in Ar + O_3	$\sim 1.5 \times 10^{16}$–8×10^{16}	~ 1.5[d]	8a
V in CO + O_3	$\sim 1.5 \times 10^{16}$–8×10^{16}	~ 2[d]	8b
Cr in Ar + O_3	$\sim 2 \times 10^{16}$–2×10^{17}	~ 1.5[d]	6a
Cr in CO + O_3	$\sim 2 \times 10^{16}$–2×10^{17}	~ 2[d]	6b
Mn in Ar + O_3	$\sim 2.5 \times 10^{16}$–2.5×10^{17}	~ 1.5[d]	7a
Mn in CO + O_3	$\sim 2.5 \times 10^{16}$–2.5×10^{17}	~ 1.5[d]	7b
Fe in He + O_3	$\sim 2 \times 10^{16}$–2×10^{17}	~ 3–8[d]	4a
Fe in CO + O_3	$\sim 2 \times 10^{16}$–2×10^{17}	$\gtrsim 2$[c]	4b
Co in Ar + O_3	$\sim 2 \times 10^{16}$–2×10^{17}	~ 1[c]	5a
Co in CO + O_3	$\sim 2 \times 10^{16}$–2×10^{17}	~ 1.2[c]	5b
Ni in Ar + O_3	$\sim 1 \times 10^{16}$–1.5×10^{17}	~ 4.3[d]	3a
Ni in CO + O_3	$\geq 1.5 \times 10^{18}$	~ 3.8[d]	3b
Ni + CO + O_3	1×10^{16}–1.5×10^{17} vaporization from Ni wire	1.5–2.5	*e*

[a] The copper and zinc systems are not sufficiently exothermic nor do they possess the low-lying electronic states for a successful application of this technique. [b] Estimated on the basis of crucible vapor pressure where appropriate. [c] Measurement of reaction chamber pressure with thermocouple gauge. [d] Measurement of reaction chamber pressure with Wallace and Tiernan gauge. [e] See text for discussion of spectrum.

Recently, there has been considerable theoretical and some experimental work directed to structural determination, the qualitative evaluation of binding energies, and the determination of relative reaction probabilities for CO adsorbed on small metal clusters.[14] The envisioned[14] simplicity of small metal clusters, compared with the complexities inherent in treating a metal surface, has been one of the prime motivating factors for the recent theoretical work, nickel being the focus of much attention. Richardson and Bradshaw[5] have determined the vibrational frequencies of the Ni_5CO cluster as a model for on-top surface site interaction and the Ni_6CO complex as a means of modeling the bridge surface site interaction. Parra and Micha[4] have recently used 9 and 14 metal atom clusters to carry out similar calculations.

Until the initial experimental work that we describe, few experimental studies had provided a direct evaluation of metal monocarbonyl binding energies.[15] Further definitive structural information with which to compare with theory has not yet been attained. Thus, there exists a need to obtain information on the binding energies and spectroscopy of metal atom and metal cluster–CO complexes.

Here, we summarize the initial phases of a study in which we compare the optical signatures of metal atom–ozone or metal atom–NO_2 reactive encounters where the metal atom is brought to the reaction zone through entrainment in either argon or carbon monoxide. In the former entrainment configuration, the metal undergoes a van der Waals interaction with argon, while in the latter, it forms carbonyl complexes in various degrees of binding.

Experimental Section

In order to study several processes involving the formation of metal atom and metal cluster complexes, we have developed a number of

---

(8) TiCO: Mortola, A. P.; Goddard, W. A., III *J. Am. Chem. Soc.* **1974**, *96*, 1–10. FeCO: Bursten, B. E.; Freier, D. G.; Fenske, R. F. *Inorg. Chem.* **1980**, *19*, 1810–1811. Guenzberger, D.; Saitovitch, E. M. B.; DePaoli, M. A.; Manela, H. *J. Chem. Phys.* **1984**, *80*, 735–744. Daoudi, A.; Suard, M.; Barbier, C. C. *C. R. Acad. Sci., Ser. 2* **1985**, *301*, 911–914. Sawaryn, A.; Aldridge, L. P.; Blaes, R.; Marathe, V. R.; Trautwein, A. *Hyperfine Interact.* **1986**, *29*, 1303–1306. NiCO: Cederbaum, L. S.; Domcke, W.; Von Niessen, W.; Brenig, W. *Z. Phys. B: Condens. Matter Quanta* **1975**, *21*, 381–388. Walch, S. P.; Goddard, W. A., III *J. Am. Chem. Soc.* **1976**, *98*, 7908–7917. Clark, D. T.; Cromarty, B. J.; Sgamellotti, A. *Chem. Phys. Lett.* **1978**, *55*, 482–487. Itoh, H.; Kunz, A. B. *Z. Naturforsch., A: Phys., Phys. Chem., Kosmophys.* **1979**, *34A*, 114–116. Bullett, D. W.; O'Reilly, E. P. *Surf. Sci.* **1979**, *89*, 274–281. Bagus, P. S.; Hermann, K. *Surf. Sci.* **1979**, *89*, 588–595. Rosen, A.; Grundevik, P.; Morovic, T. *Surf. Sci.* **1980**, *95*, 477–495. Rives, A. B.; Weinhold, F. *Int. J. Quantum Chem., Quantum Chem. Symp.* **1980**, *14*, 201–209. Saddei, D.; Freund, H. J.; Hohlmeicher, G. *Chem. Phys.* **1981**, *55*, 339–354. Howard, I. A.; Pratt, G. W.; Johnson, K. H.; Dresselhaus, G. *J. Chem. Phys.* **1981**, *74*, 3415–3419. Rives, A. B.; Fenske, R. F. *J. Chem. Phys.* **1981**, *75*, 1293–1302. McIntosh, D. F.; Ozin, G. A.; Messmer, R. P. *Inorg. Chem.* **1981**, *20*, 3640–3650. Bagus, P. S.; Roos, B. O. *J. Chem. Phys.* **1981**, *75*, 5961–5962. Dunlap, B. I.; Yu, H. L.; Antoniewicz, P. R. *Phys. Rev. A* **1982**, *25*, 7–13. You, X. *Jiegou Huaxue* **1983**, *2*, 183–188. Huzinaga, S.; Klobukowski, M.; Sakai, Y. *J. Phys. Chem.* **1984**, *88*, 4880–4886. Ha, T. K.; Nguyen, M. T. *THEOCHEM* **1984**, *18*, 331–338. Rohlfing, C. M.; Hay, P. J. *J. Chem. Phys.* **1985**, *83*, 4641–4649. Kao, C. M.; Messmer, R. P. *Phys. Rev. B* **1985**, *31*, 4835–4847. Bauschlicher, C. W., Jr. *J. Chem. Phys.* **1986**, *84*, 260–267. Carsky, P.; Dedieu, A. *Chem. Phys.* **1986**, *103*, 265–275. CuCO: Itoh, H.; Kunz, A. *Z. Naturforsch., A: Phys., Phys. Chem., Kosmophys.* **1979**, *34A*, 114–116. McIntosh, D. F.; Ozin, G. A.; Messmer, R. P. *Inorg. Chem.* **1981**, *20*, 3640–3650. Ha, T. K.; Nguyen, M. T. *THEOCHEM* **1984**, *18*, 331–338. Kuzminskii, M. B.; Bagaturyants, A. A.; Kazanskii, V. B. *Izv. Akad. Nauk. SSSR, Ser. Khim.* **1986**, 284–288.

(9) VCO: Hanlan, L.; Huber, H.; Ozin, G. A. *Inorg. Chem.* **1976**, *15*, 2592–2597. Van Zee, R. J.; Bach, S. B. H.; Weltner, W., Jr. *J. Phys. Chem.* **1986**, *90*, 583–588. CrCO: Ozin, G. A., Vander Voet, A. *Prog. Inorg. Chem.* **1975**, *19*, 137. MnCO: Huber, H.; Kundig, E. P.; Ozin, G. A.; Poe, A. J. *J. Am. Chem. Soc.* **1975**, *97*, 308–314. Lichtin, D. A.; Bernstein, R. B.; Vaida, V. *J. Am. Chem. Soc.* **1982**, *104*, 1830–1834. FeCO: *Cryochemistry*; Ozin, G. A., Moskovits, M., Eds.; Wiley: New York, 1986. Engelking, P. C.; Lineberger, W. C. *J. Am. Chem. Soc.* **1979**, *101*, 5569–5573. Peden, C. H. F.; Parker, S. F.; Barrett, P. H.; Pearson, R. G. *J. Phys. Chem.* **1983**, *87*, 2329–2336. CoCO: Hanlan, L. A.; Huber, H.; Kuendig, E. P.; McGarvey, B. R.; Ozin, G. A. *J. Am. Chem. Soc.* **1975**, *97*, 7054–7068. NiCO: DeKock, R. L. *Inorg. Chem.* **1971**, *10*, 1205–1211. Kuendig, E. P.; McIntosh, D.; Moskovits, M.; Ozin, G. A. *J. Am. Chem. Soc.* **1973**, *95*, 7234–7241. Garrison, B. J.; Winograd, N.; Harrison, D. E., Jr. *J. Vac. Sci. Technol.* **1979**, *16*, 789–792. Stevens, A. E.; Feigerle, C. S.; Lineberger, W. C. *J. Am. Chem. Soc.* **1982**, *104*, 5026–5031. CuCo: Huber, H.; Kuendig, E. P.; Moskovits, M.; Ozin, G. A. *J. Am. Chem. Soc.* **1975**, *97*, 2097–2106. Garrison, B. J.; Winograd, N.; Harrison, D. E., Jr. *J. Vac. Sci. Technol.* **1979**, *16*, 789–792. Kasai, P. H.; Jones, P. M. *J. Am. Chem. Soc.* **1985**, *107*, 813–818.

(10) Moskovits, M. "Application of Matrix Isolation to the Study of Metal Clusters with a Postscript on the Reactivity of Clusters in Supersonic Beams". *Metal Clusters*; Moskovits, M., Ed.; Wiley: New York, 1986; p 185.

(11) Hulse, J. E.; Moskovits, M. *Surf. Sci.* **1976**, *57*, 125.

(12) Moskovits, M.; Hulse, J. E. *J. Phys. Chem.* **1977**, *81*, 2004.

(13) Moskovits, M. *Acc. Chem. Res.* **1979**, *12*, 229.

(14) Morse, M. D.; Geusic, M. E.; Heath, J. R.; Smalley, R. E. *J. Chem. Phys.* **1985**, *83*, 2293.

(15) Stevens, A. E.; Feigerle, C. S.; Lineberger, W. C. *J. Am. Chem. Soc.* **1982**, *104*, 5026.

"variable flux" continuous metal flow entrainment sources. A typical agglomeration-entrainment device is depicted schematically in Figure 1.[16,17] Here, using a tungsten basket heater (R. D. Mathis), a metal is heated in a particularly designed crucible to temperatures producing a metal vapor pressure that can range to 3 orders of magnitude greater than that employed for effusive operation.[16,17] The basket heater is wrapped in zirconia cloth (Zircar, Florida, NY) and surrounded concentrically by (1) a tantalum heat shield and (2) a cylindrical heavy-walled zirconia tube (Zircar). Both the top and bottom of the basket heater zone are heavily insulated with zirconia cloth. This extra insulation allows the ready operation of the tungsten basket heater at temperatures consistently at the upper limits of its performance specifications.

At the lowest fluxes, we entrain substantial concentrations of metal atoms in an appropriate carrier gas. While this carrier gas might be helium or argon, which interacts weakly with the metal (e.g. van der Waals interaction), the approach that we pursue in the study outlined here uses an entrainment gas capable of forming a complex with the metal atom. Subsequently, the entrained "complexing" metal mixture is oxidized to obtain information on the metal atom–entrainment gas binding energy through chemiluminescent studies of a final metal oxide product and to study the chemiluminescence from metal oxide complexes formed in the oxidation reaction.

In this study, the transition metals were heated in specifically designed crucibles to temperatures between 1350 and 2400 K, producing a vapor pressure ranging from 10^{-2} to 10^{-1} Torr for most of the experiments considered here (see Table I). The metal flux issuing from the lower crucible chamber is entrained in a rare gas or CO flow ranging in pressure from 100 to approximately 5000 mTorr, dependent upon the metal under study and the optimization of those (chemiluminescent) oxidation processes under study. Before it is brought to the entrainment zone, the carbon monoxide (Matheson, 99.5%) passes through a copper coil immersed in a dry ice–methanol slush bath to trap any metal carbonyls that may have formed in the carbon monoxide cylinder. At a suitable point above the flow, an oxidant intersects the entrained metallic flow, entering usually from a concentric ring injector inlet or from a nozzle perpendicular to the flow and elevated above the cooled upper region of the oven assembly. Typical oxidant pressures ranged from 10 to 40 mTorr.

There are a number of factors including metallic flux, entrainment gas cooling rate, pumping speed, and oxidant configuration that determine the nature of the species that can be formed and whose reaction or complexing can be probed employing fluorescence spectra that can be generated by the techniques outlined. A process must be of sufficient exothermicity to populate the excited electronic states of the products of a probing reaction, be they polyatomic or diatomic emitters. A significant limiting factor to the success of the experiments we describe is the magnitude of the quantum yield[18] for fluorescence once the excited electronic states of the diatomic or polyatomic product molecules on which we will focus are populated. This will be influenced by transition moments, the strength of coupling to nonradiative channels, and the density of product states as it increases with atomic mass. Thus, in a given system, there will be a number of conditions that must be varied to produce optimal cluster distributions for dissociative oxidation to form the emitting transition-metal oxides (binding energies) or the corresponding oxide–CO complexes.

The chemiluminescence from the reactions of interest was observed at right angles to the metal flow. Spectral emissions were monitored with a 1-m Spex 1704 monochromator operated in first order with a Bausch and Lomb grating blazed at 5000 Å. A dry ice cooled EMI 9808 photomultiplier tube detected the dispersed fluorescence and provided a signal for a Keithley 417 fast picoammeter whose output signal, partially damped, drove a Leeds and Northrup strip chart recorder on which the spectra were recorded. All spectra were wavelength calibrated.

Results

Metal Carbonyl Binding Energies. In the first phase of our efforts, we have performed a series of comparative oxidation experiments that are well exemplified by the data in Figure 2 for the titanium (Ti) atom oxidation system. We can generate a Ti atom flux from an oven-based crucible design or, in an alternate configuration, we vaporize Ti from a filament formed through vapor deposition of the titanium metal onto a molybdenum base. The data presented in Figure 2 were obtained using the filament-based configuration. The lower spectrum in Figure 2 corresponds to emission from several excited states of titanium oxide (TiO) formed when Ti atoms vaporized from a molybdenum filament and entrained in argon are subsequently oxidized with ozone. Hence, we observe the signature of the process in eq 1

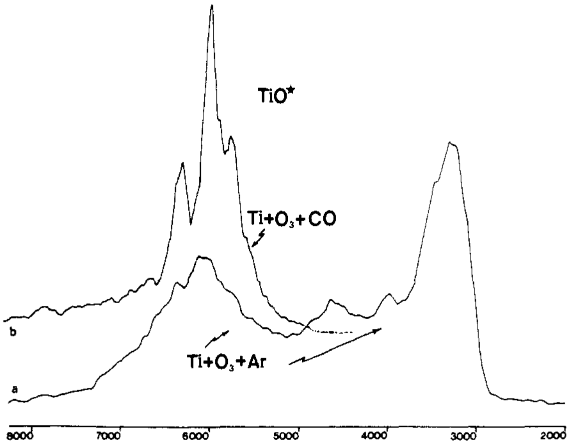

Figure 2. Chemiluminescent spectra for the multiple-collision oxidation of titanium atoms with ozone to form the excited states of titanium oxide. (a) Spectrum obtained when titanium atoms vaporized from a molybdenum-based filament and entrained in argon ($Ti + O_3 + Ar \rightarrow TiO^* + O_2 + Ar$) are oxidized to yield a spectrum onsetting at 2900 Å; $P_{total}(Ar) \approx 2$ Torr. (b) Spectrum obtained when titanium atoms vaporized from a molybdenum-based filament and entrained in CO ($Ti + O_3 + CO \rightarrow TiCO + O_3 \rightarrow TiO^* + CO + O_2$) are oxidized to yield a spectrum onsetting at 4920 Å; $P_{total}(CO) \approx 2.5$ Torr. Spectral resolution for both scans is 12 Å. See text for discussion.

$$Ti + O_3 + Ar \rightarrow TiO^* + O_2 + Ar \qquad (1)$$

under multiple-collision conditions. The short-wavelength limit of the spectrum in Figure 2 is determined by the exothermicity of reaction 1. The upper trace in Figure 2 corresponds to the observed emission spectrum when the entrainment gas is switched to carbon monoxide. Here, the observed TiO emission onsets at considerably longer wavelength. This situation results because the oxidation processes now correspond to the sequence in eq 2

$$Ti + xCO \rightarrow Ti(CO)_x \qquad (2a)$$

$$Ti(CO)_x + O_3 \rightarrow TiO^* + O_2 + xCO \qquad (2b)$$

where the exothermicity of that process forming TiO* is diminished by the magnitude of the total M–CO binding energy. In fact, the sequence of reaction 2 is found to take place at notably lower filament temperature. CO interacting with the filament-deposited titanium may create a more volatile MCO species, which vaporizes at a somewhat lower temperature than the titanium.

On the basis of the above considerations, it is apparent that the difference in spectral wavelength onset for the TiO emissions in Figure 2 can be used to obtain a value for the Ti–CO binding energy. We find

$$E_{binding} = E_{2900Å}\ (34\,473\ cm^{-1}) - E_{4920Å}\ (20\,320\ cm^{-1}) = 14\,150\ cm^{-1}\ (1.75\ eV)$$

Similar results are obtained by using an oven-based configuration with nickel atoms entrained in argon and CO. Here, the $Ni + O_3 + Ar$ system yields an NiO emission spectrum onsetting at 4480 Å whereas the $Ni + CO + O_3 \rightarrow NiO^* + O_2 + CO$ configuration operated at high nickel flux behaves very differently and yields a weaker NiO emission onsetting at ≈7500 Å (Figure 3). The difference in these two onsets gives a measure of the Ni–CO binding energy, $E \approx 9000\ cm^{-1}$ (1.12 eV). This value

---

(16) For example, see: Preuss, D. R.; Gole, J. L. *J. Chem. Phys.* **1977**, *66*, 2994. Gole, J. L.; Preuss, D. R. *J. Chem. Phys.* **1977**, *66*, 3000. Dubois, L. H.; Gole, J. L. *J. Chem. Phys.* **1977**, *66*, 779. Lindsay, D. M.; Gole, J. L. *J. Chem. Phys.* **1977**, *66*, 3886. Gole, J. L.; Pace, S. A. *J. Chem. Phys.* **1980**, *73*, 836. Chalek, C. L.; Gole, J. L. *J. Chem. Phys.* **1976**, *65*, 2845. Gole, J. L.; Pace, S. A. *J. Phys. Chem.* **1981**, *65*, 2651. Gole, J. L. *Annu. Rev. Phys. Chem.* **1976**, *27*, 525. Green, G. J.; Gole, J. L. *Chem. Phys.* **1985**, *100*, 133. Woodward, R.; Hayden, J. S.; Gole, J. L. *Ibid.* **1985**, *100*, 153.

(17) Woodward, R.; Le, P. N.; Temmen, M.; Gole, J. L. *J. Phys. Chem.* **1987**, *91*, 2637.

(18) Bauschlicher, C. W., Jr.; Bagus, P. S.; Nelin, C.; Roos, B. O. *J. Chem. Phys.* **1986**, *85*, 354.

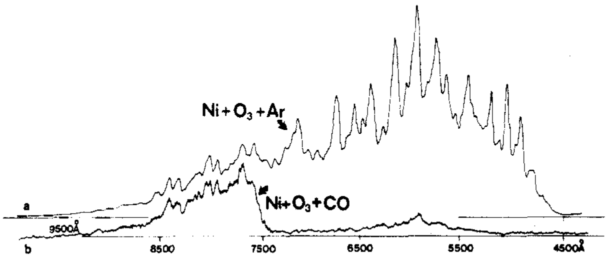

Figure 3. Chemiluminescent spectra for the multiple-collision oxidation of nickel atoms with ozone to form the excited states of nickel oxide. (a) Spectrum obtained when nickel atoms entrained in argon ($Ni + O_3 + Ar \rightarrow NiO^* + O_2 + Ar$) are oxidized to yield a spectrum onsetting at 4480 Å; $P_{total}(Ar) \approx 4.3$ Torr. (b) Spectrum obtained when a high flux of nickel atoms entrained in CO ($Ni + O_3 + CO \rightarrow NiCO + O_3 \rightarrow NiO^* + O_2 + CO$) is oxidized to yield a spectrum onsetting at ≈7500 Å; $P_{total}(CO) \approx 3.8$ Torr. Spectral resolution for both scans is 12 Å. Spectrum b is taken at a sensitivity approximately 10 times that of spectrum a. See Table I and text for discussion.

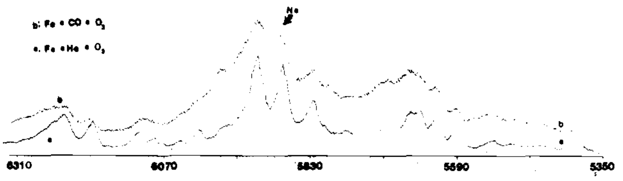

Figure 4. Chemiluminescent spectra for the multiple-collision oxidation of iron atoms entrained in helium or carbon monoxide. (a) Iron atoms entrained in helium are oxidized ($Fe + O_3 + He \rightarrow FeO^* + O_2 + He$) to yield the FeO emission spectrum. $P_{total}(He) \approx 3$–8 Torr. (b) Iron atoms entrained in CO form a metal carbonyl complex, which is then oxidized ($Fe + xCO + O_3 \rightarrow FeCO + yCO + O_3 \rightarrow FeOCO^* + O_2 + yCO$) to form an electronically excited metal oxide carbonyl complex whose optical signature is monitored; $P_{total}(CO) \approx 2$ Torr. Spectral resolution is 10 Å for both scans a and b. See Table I and text for discussion.

is in excellent agreement with the calculations of Bauschlicher et al.[18] for $^1\Sigma^+$ NiCO ($D_e = 1.10$ eV).

Weakly Bound Electronically Excited Metal Oxide–CO Complexes Formed in Metal-Based Oxidations. On the basis of our successes with the titanium and nickel systems, we felt it appropriate to examine the remainder of the first-row transition elements. The results of our initial studies display an intriguing trend associated with the molecular electronic structure and strength of the metal carbonyl bond. Here, we consider the emission spectra associated with the oxidation of Fe, Co, Cr, Ni, Mn, Sc, and V where these metal atoms are entrained in both Ar or He and CO and subsequently oxidized under the conditions summarized in Table I. In Figure 4 we present the optical signatures that result when iron is entrained in helium or CO and subsequently oxidized with O_3 to produce emission spectra that, for helium entrainment, are attributable to FeO. In comparing to the helium spectrum, we find that the emission that characterizes the ($Fe + xCO$) – O_3 oxidation system does not display the sharp changes in the electronic emission or excited-state vibrational distribution found under those conditions that we have exemplified in our studies of the Ti and Ni systems (entrained in Ar and CO; see Discussion). Rather, the "$Fe + xCO$" emission spectrum would appear to show little evidence of a substantial change in the "FeO" excited-state vibrational population distribution versus the emission characterizing the Fe + helium oxidation system. A further, at first puzzling, factor in the iron systems is the clear broadening of spectral features for the spectrum obtained with CO entrainment versus that obtained with helium entrainment. Similar results are obtained for the cobalt systems whose signatures for the ozone oxidation of argon- and CO-entrained atomic cobalt are depicted in Figure 5. Here, sharp features clearly observed in the argon spectrum are apparently washed into a broad almost continuous overall emission feature. This seeming indication of an enhanced rotational excitation is puzzling since CO should be a much more effective collisional relaxant than argon or helium. In fact, we now believe that the broadening of the "CO" spectra in Figures 4 and 5 signals the formation of a relatively long-lived excited-state metal oxide carbonyl complex whose radiative lifetime may be on the order of 10^{-7} s.

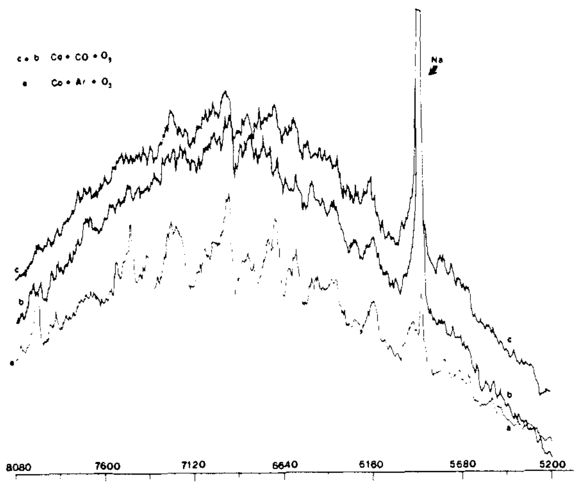

Figure 5. Chemiluminescent spectra for the multiple-collision oxidation of cobalt atoms entrained in argon or carbon monoxide. (a) Cobalt atoms entrained in argon are oxidized ($Co + O_3 + Ar \rightarrow CoO^* + O_2 + Ar$) to yield the CoO emission spectrum. $P_{total}(Ar) \approx 1$ Torr. (b) Cobalt atoms entrained in CO form a metal carbonyl complex, which is then oxidized ($Co + xCO + O_3 \rightarrow CoCO + yCO + O_3 \rightarrow CoOCO^* + O_2 + yCO$) to form an electronically excited metal oxide carbonyl complex whose optical signature is monitored; $P_{total}(CO) \approx 1.2$ Torr. Spectral resolution is 15 Å for both scans a and b. See Table I and text for discussion.

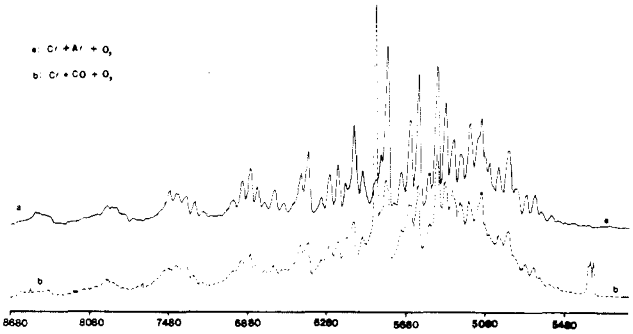

Figure 6. Chemiluminescent spectra for the multiple-collision oxidation of chromium atoms entrained in argon or carbon monoxide. (a) Chromium atoms entrained in argon are oxidized ($Cr + O_3 + Ar \rightarrow CrO^* + O_2 + Ar$) to yield the CrO emission spectrum. $P_{total}(Ar) \approx 1.5$ Torr. (b) Chromium atoms entrained in CO form a metal carbonyl complex, which is then oxidized ($Cr + xCO + O_3 \rightarrow CrCO + yCO + O_3 \rightarrow CrOCO^* + O_2 + yCO$) to form an electronically excited metal oxide carbonyl complex whose optical signature is monitored; $P_{total}(CO) \approx 2$ Torr. Spectral resolution is 10 Å for both scans a and b. See Table I and text for discussion.

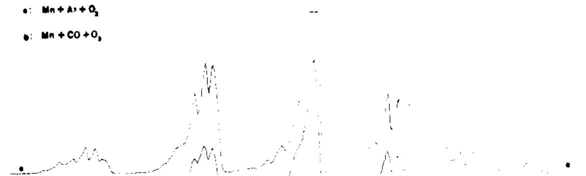

Figure 7. Chemiluminescent spectra for the multiple-collision oxidation of manganese atoms entrained in argon or carbon monoxide. (a) Manganese atoms entrained in argon are oxidized ($Mn + O_3 + Ar \rightarrow MnO^* + O_2 + Ar$) to yield the MnO A–X emission spectrum; $P_{total}(Ar) \approx 1.5$ Torr. (b) Manganese atoms entrained in CO are oxidized ($Mn + O_3 + CO \rightarrow MnO^* + O_2 + CO$) to yield the MnO A–X emission spectrum; $P_{total}(CO) \approx 1.5$ Torr. Spectral resolution is 7.5 Å for both scans a and b. See Table I and text for discussion.

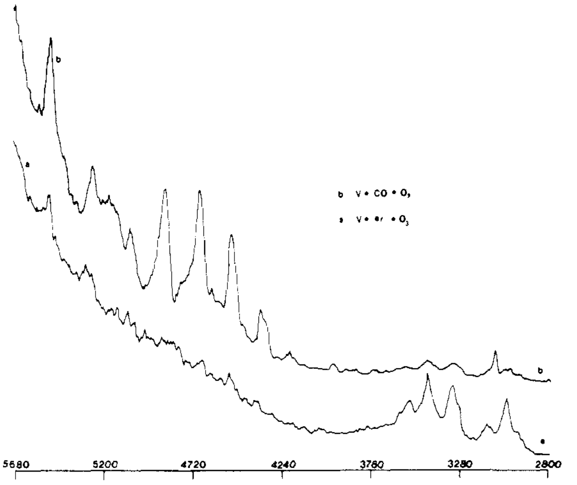

Figure 8. Chemiluminescent spectra for the multiple-collision oxidation of vanadium atoms entrained in argon or carbon monoxide. (a) Vanadium atoms entrained in argon are oxidized ($V + O_3 + Ar \rightarrow VO^* + O_2 + Ar$) to yield the VO emission spectrum. $P_{total}(Ar) \approx 1.5$ Torr. (b) Vanadium atoms entrained in CO form a metal carbonyl complex, which is then oxidized ($V + xCO + O_3 \rightarrow VCO + yCO + O_3 \rightarrow VOCO^* + O_2 + yCO$) to form an electronically excited metal oxide carbonyl complex whose optical signature is monitored; $P_{total}(CO) \approx 2$ Torr. Spectral resolution is 20 Å for both scans a and b. See Table I and text for discussion.

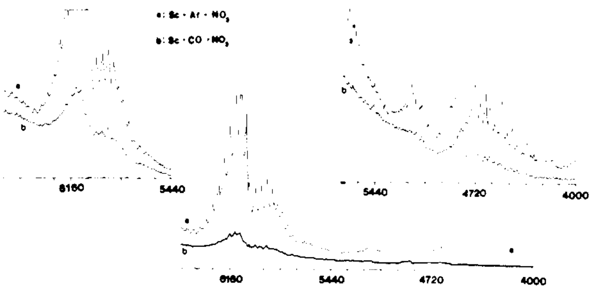

Figure 9. Chemiluminescent spectra for the multiple-collision oxidation of scandium atoms entrained in argon or carbon monoxide. (a) Scandium atoms entrained in argon are oxidized ($Sc + NO_2 + Ar \rightarrow ScO^* + NO + Ar$) to yield the ScO emission spectrum. $P_{total}(Ar) \approx 0.8$ Torr. (b) Scandium atoms entrained in CO form a metal carbonyl complex, which is then oxidized ($Sc + xCO + O_3 \rightarrow ScCO + yCO + O_3 \rightarrow ScOCO^* + O_2 + yCO$) to form an electronically excited metal oxide carbonyl complex whose optical signature is monitored; $P_{total}(CO) \approx 1$ Torr. Spectral resolution is 7 Å for both scans a and b. See Table I and text for discussion.

Much less pronounced broadening is noted with CO entrainment in the chromium oxidation system (Figure 6) and for the nickel oxidation system under CO-entrainment conditions, which differ (Table I) from those required to obtain a cutoff due to the change in reaction exoergicity as a relaxed nickel carbonyl complex is oxidized (Figure 3). Much more substantial complexing effects are found in comparing argon versus CO-entrained spectra for the vanadium and scandium systems (Figures 8 and 9) where the sizable increase in the metal oxide bond strength for the beginning transition elements may play an important role in stabilizing the carbonyl complex.

Recently, Weltner, Vala, and co-workers[19] have examined infrared and ESR matrix isolation studies of the transition-metal monocarbonyls. These authors summarize the very intriguing correlations presented in Figure 10 in which a comparison between CO stretching frequencies, ν_{CO}, and the variation of promotion energies for the first-row transition metals is presented. Here, deviations of the CO stretching frequency from that of naked CO, $\nu_{CO} \approx 2140$ cm^{-1}, provide an indication of the strength of the M–C bond, and it is reasoned that a close correlation exists with increased deviation and bond strength. One notes substantial deviations from $\nu_{CO} \approx 2140$ cm^{-1} with the exception of manganese, the correlations thus implying that Mn–CO is nonbonded. This result bears an outstanding correlation with the manganese spectra presented in Figure 6. Here broadening effects in the CO-entrained manganese oxidation spectrum are virtually absent versus the signatures of the argon-entrained system. In fact, the spectrum for the CO-entrained $Mn–O_3$ oxidation system appears to be more rotationally relaxed than that of the argon-entrained $Mn–O_3$ system. This is precisely the expected result if CO acts as a more effective relaxant in a spectator role.

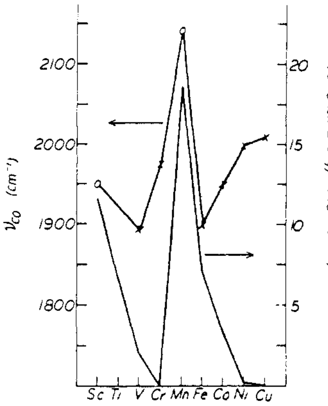

Figure 10. Plot of the CO stretching frequencies for the first-row transition-metal monocarbonyl molecules MCO (circled points are tentative) and variation of promotion energy corresponding to $4s^23d^{n-2} \rightarrow 4s^13d^{n-1}$, where n is the number of valence electrons.

In summary, we have evidence for transition-metal oxide carbonyl complex formation in the presence of a significant M–CO bond and a complete absence of broadening effects, which signal complex formation when M–CO bonding is apparently nonexistent. There is a strong correlation between the spectral data summarized here (Figures 4–9) and the trends depicted in Figure 10.

Discussion

We have tentatively identified metal oxide carbonyl complex emissions. The observations outlined here bear some complement to recent studies of collision complexes and the transition state in molecular beams, heat pipe ovens, and bulb experiments.[20] There are many factors that need to be investigated and assessed to better understand the formation of these relatively long-lived excited electronic states[21] and the precise nature of the observed emission spectra (Figures 4–9). We are observing emissions from systems where the excited-state binding to CO is sufficient to accommodate the energy flow in moderate to highly exothermic

---

[19] Bach, S. B. H.; Taylor, C. A.; Van Zee, R. J.; Vala, M. T.; Weltner, W., Jr. *J. Am. Chem. Soc.* **1986**, *108*, 7104.

[20] For example, see: Kleiber, P. D.; Lyyra, A. M.; Sands, K. M.; Zafiropulos, V.; Stwalley, W. C. *J. Chem. Phys.* **1986**, *85*, 5493. Also: (a) Gallagher, A. In *Spectral Line Shapes*; Burnett, K., Ed.; de Gruyter: Berlin, 1982; Vol. II, p 755. (b) Polanyi, J. C. *Faraday Discuss. Chem. Soc.* **1979**, *67*, 129. (c) Arrowsmith, P.; Bly, S. H. P.; Charters, P. E.; Polanyi, J. C. *J. Chem. Phys.* **1983**, *79*, 283. Arrowsmith, P.; Bartoszek, P. E.; Bly, S. H. P.; Carrington, T., Jr.; Charters, P. E.; Polanyi, J. C. *Ibid.* **1980**, *73*, 5895. (d) Hering, P.; Brooks, P. R.; Curl, R. F., Jr.; Judson, R. S.; Lowe, R. S. *Phys. Rev. Lett.* **1980**, *44*, 687. Maguire, T. C.; Brooks, P. R.; Curl, R. F., Jr. *Ibid.* **1983**, *50*, 1918. (e) Kleiber, P. D.; Lyyra, A. M.; Sando, K. M.; Heneghan, S. P.; Stwalley, W. C. *Phys. Rev. Lett.* **1985**, *54*, 2003. (f) Breckenridge, W. H.; Umemoto, H. *J. Chem. Phys.* **1981**, *75*, 698. (g) Breckenridge, W. H.; Umemoto, H. *J. Chem. Phys.* **1984**, *80*, 4168, and references therein.

[21] From the experiments conducted thus far, we cannot unequivocally rule out the possibility that the observed optical signature mirrors the effect of a sticky complex dissociation as the CO separates from the transition metal during the oxidation process. However, we believe that the data are more consistent with a complex that maintains the transition-metal–CO bond during the oxidation and emission process. If we observe the effects of the dissociation of a sticky complex, energy conservation dictates that the M–CO molecule must be internally excited to an energy that is close to that required for dissociation of the metal–carbonyl bond. In view of the multiple-collision environment in which the carbonyl is formed and entrained, this seems an unlikely possibility.

oxidation processes for time scales, which should be comparable to the metal oxide excited-state radiative lifetime.[21] The ability to accommodate the energy flow depends on several excited-state parameters and system conditions, which will be the subject of further evaluation.

Several factors must be varied in these systems (Table I) in order to provide (1) the opportunity to observe complex formation and (2) a clear definition of spectral cutoff and the conditions that establish this cutoff so as to further evaluate metal cluster binding energies. We are currently investigating the conditions that lead to the most effective complexing and how the variation of experimental parameters can be exploited to study the complex itself. In the evaluation of spectral cutoffs, we will need to assess whether the M–CO vibrational mode can be completely relaxed to a Boltzmann or well-defined distribution before reaction occurs. We must evaluate whether there will be a sufficient number of vibrationless MCO species so that the differences in spectral onset can be used to evaluate a more precise *lower bound* to the binding energy. Further, the question of whether the dissociation processes (eq 2) produce some vibrationless ground state or exclusively vibrationally excited CO must be considered. If the CO, which dissociates from a vibrationally relaxed complex during oxidation, is vibrationally excited, then the differential energy increment does not reflect the magnitude of the M–$(CO)_x$ binding energy but, in fact, may overestimate this quantity as a decrease in the ultimate MO* excited-state excitation must result. If the M–CO complex is not vibrationally relaxed, the energy available within the complex may tend to mute the full magnitude of the M + O_3 and $M(CO)_x$ + O_3 energy differences (onsets for electronic emission will not differ by the binding energy), leading to a lower bound evaluation of the binding energy. Although we do not feel that this correction represents a major factor in the Ti and Ni systems, we must also be concerned with the nature of those Franck–Condon factors, which relate the levels of those ground and excited states of the emitting metal oxide molecules whose optical signatures are monitored in this study. The energy cutoffs may be related to energy content in different ways when different electronic states or systems are involved, and these changes must certainly be taken into account. With further parameterization, it should also be possible to evaluate the nature of those ground states to which emission occurs in these systems by a judicious combination of chemiluminescent and mass spectrometric techniques.

Our estimate of the radiative lifetime of the emitting complexes ($\sim 10^{-7}$ s) is based on a comparison with the limited data base available for the transition-metal oxides.[21] Parson et al.[22] have measured the radiative lifetimes for several vibrational levels of the ScO $A^2\Pi$ and $B^2\Sigma^+$ states finding $\tau_{A^2\Pi(v=0)} \approx 30$ ns and $\tau_{B^2\Sigma^+} \approx 30$–40 ns. Similarly, Johnson[23] has measured a 100-ns radiative lifetime for the FeO 5000-Å system (Figure 3), Feinberg et al.[24] have measured a radiative lifetime of 19.5 ns for the TiO $c'1\Phi$–$a^1\Delta$ transition, and certain VO transitions ($c^4\Sigma^-$–$X^4\Sigma^-$) are thought to have lifetimes on the order of 100 ns.[25]

On the basis of these limited available data and the assumption that the radiative lifetime of the emitting complex[21] should be at least comparable to that of the diatomic metal oxide, we estimate that the metal oxide carbonyl complexes must live for a time period ranging from a minimum of 5×10^{-8} s,[21] hence, the estimate $\sim 10^{-7}$ s. This, of course, corresponds to a time frame considerably longer than that expected for an excited-state van der Waals complex,[26] suggesting at least a moderate chemical binding of the solvating carbonyl group to the metal oxide. In other words, we begin to observe the formation and behavior of systems lying intermediate to van der Waals complexes and chemically bound polyatomic emitters.

There are few comparisons that can be made with our determined binding energies at present; however, NiCO does represent one exception. In studying the laser photoelectron spectrum of $NiCO^-$, Stevens et al.[15] have determined an Ni–CO bond energy of 29 ± 15 kcal/mol (1.26 ± 0.65 eV). Bauschlicher et al.[18] in an elegant ab initio calculation have determined a value of 1.10 eV for the bond energy of $^1\Sigma^+$ NiCO. Thus, our current determination of the lower bound to the NiCO bond energy is in good agreement with both previous experimental and recent theoretical determinations.

The initial results outlined here and recent results obtained for the $Al(CO)_x$ and $Al(CO_2)_x$ systems[27] indicate that we will be able to (1) establish $M(CO)_x$ ($x = 1, 2$) (and possibly $M(CO_2)_x$ ($x = 1, 2$))[27] transition-metal binding energies from chemiluminescent onsets, (2) study long-lived electronic emissions from metal oxide carbonyl complexes formed in metal carbonyl complex oxidation, and (3) approach the spectroscopy of M–CO complexes. These metal atom based solvation complexes represent a sparsely studied middle ground region extending in various degrees from weak binding van der Waals interactions to strong chemical bonding.

The data obtained thus far for these transition-metal CO systems suggest that CO solvation and complex formation present only a small perturbation on the electronic spectra of the metal oxide. Not only do these results indicate that we are dealing with a relatively weak interaction of the CO with the molecular electronic structure of the metal oxide, producing essentially a highly perturbed metal oxide excited electronic state, but also they suggest that the *spectra of the $M(CO)_x$ complexes can be observed through a variety of spectrosopies in the vicinity of known atomic transitions for the metal atoms of interest.*

While our primary focus has been on metal atom CO complexes, these studies can be extended to the corresponding metal cluster compounds $M_x(CO)_y$ ($x = 1, 2, ...; y = 1, 2$).[28] We believe that such studies will contribute to the understanding of metal carbonyl chemistry.

Registry No. Sc, 7440-20-2; Ti, 7440-32-6; V, 7440-62-2; Cr, 7440-47-3; Mn, 7439-96-5; Fe, 7439-89-6; Co, 7440-48-4; Ni, 7440-02-0; NO_2, 10102-44-0; O_3, 10028-15-6; Ar, 7440-37-1; CO, 630-08-0; He, 7440-59-7; TiO, 12137-20-1; NiO, 1313-99-1; FeO, 1345-25-1; CoO, 1307-96-6; CrO, 12018-00-7; MnO, 1344-43-0; VO, 12035-98-2; ScO, 12059-91-5; TiCO, 51286-39-6; NiCO, 33637-76-2; FeCO, 71701-40-1; CoCO, 58168-84-6; CrCO, 63375-39-3; VCO, 59982-45-5; ScCO, 99351-61-8; FeOCO, 115160-89-9; CoOCO, 115160-90-2; CrOCO, 115160-91-3; VOCO, 115160-92-4; ScOCO, 115160-93-5.

---

(22) Liu, K.; Parson, J. M. *J. Chem. Phys.* **1977**, *67*, 1814. Parson, J. M., private communication.

(23) Johnson, S. E. Ph.D. Thesis, University of California, Santa Barbara, CA, 1971.

(24) Feinberg, B.; Davis, S. P.; Phillips, J. G. *Appl. Phys. Lett.* **1976**, *12*, 147. Feinberg, B.; Davis, S. P. *J. Molec. Spectros.* **1977**, *65*, 264.

(25) Parson, J., private communication.

(26) Levy, D. H. *Adv. Chem. Phys.* **1981**, *47*, 323. Janda, K. C. *Adv. Chem. Phys.* **1985**, *60*, 201. Celii, F. E.; Janda, K. C. *Chem. Rev.* **1986**, *86*, 507.

(27) McQuaid, M.; Woodward, J. R.; Gole, J. L. *J. Phys. Chem.* **1988**, *92*, 252–255.

(28) Gole, J. L.; Bondybey, V.; English, J. H. *J. Phys. Chem.* **1982**, *86*, 2560. Gole, J. L. *Adv. Laser Sci.—2*, in press.